Available online at www.sciencedirect.com
SCIENCE DIRECT®
C. R. Mecanique 332 (2004) 403–411
COMPTES RENDUS MECANIQUE

Microgravity and Transfers/Solidification, crystal growth from the melt

Modelling of binary alloy solidification in the MEPHISTO experiment

Eddie Leonardi [a,*], Graham de Vahl Davis [a], Victoria Timchenko [a], Peter Chen [a], Reza Abbaschian [b]

[a] *School of Mechanical and Manufacturing Engineering, The University of New South Wales, Sydney, NSW 2052, Australia*
[b] *Department of Materials Science and Engineering, University of Florida, Gainesville, FL 32611, USA*

Available online 24 April 2004

Abstract

A modified enthalpy method was used to numerically model experiments on solidification of a bismuth-tin alloy which were performed during the 1997 flight of the MEPHISTO-4 experiment on the US Space Shuttle Columbia. This modified enthalpy method was incorporated into an in-house code SOLCON and a commercial CFD code CFX; Soret effect was taken into account by including an additional thermo-diffusion term into the solute transport equation and the effects of thermal and solutal convection in the microgravity environment and of concentration-dependent melting temperature on the phase change processes were also included. In this paper an overview of the results obtained as part of MEPHISTO project is presented. The numerical solutions are compared with actual microprobe results obtained from the MEPHISTO experiment. ***To cite this article: E. Leonardi et al., C. R. Mecanique 332 (2004).***

Résumé

Modélisation de la solidification d'un alliage binaire dans le dispositif expérimental MEPHISTO. Une méthode enthalpique est adaptée pour la modélisation d'une expérience de solidification dirigée de l'alliage bismuth-étain qui a eu lieu en 1997 durant le vol du dispositif MEPHISTO-4 embarqué dans la navette spatiale américaine Columbia. Ce modèle a été implémenté conjointement dans un code du laboratoire SOLCON et dans le code commercial CFX. L'effet Soret a été pris en compte en introduisant des termes de thermo-diffusion additionnels dans l'équation de transport solutal. Les effets de la convection thermique et solutale en microgravité ainsi que ceux de la température de changement de phase qui est une fonction de concentration ont également été pris en compte. Dans cet article une revue des résultats faisant partie du projet MEPHISTO est présentée. Les solutions numériques sont comparées aux relevés expérimentaux. ***Pour citer cet article : E. Leonardi et al., C. R. Mecanique 332 (2004).***

Keywords: Heat transfer; Solidification; Microgravity; MEPHISTO experiment

Mots-clés : Transferts thermiques ; Solidification ; Microgravité ; Expérience MEPHISTO

* Corresponding author.
E-mail address: E.Leonardi@unsw.edu.au (E. Leonardi).

1631-0721/$ – see front matter
doi:10.1016/j.crme.2004.02.010

1. Introduction

In the last decade experiments on solidification have been conducted in a microgravity environment where convection can be decreased to a level at which crystal growth is largely diffusion controlled and therefore fundamental aspects of crystal growth can be studied. One example of such studies is the MEPHISTO[1] program, a cooperative US–French–Australian research effort directed towards gaining a detailed understanding of crystal growth with reference to the solidification behaviour of Bi-1 at % Sn alloy. The latest MEPHISTO experiment was performed on board the US Space Shuttle *Columbia* during the USMP-4 mission in November–December 1997 [1].

A numerical study of the MEPHISTO experiment has become an important part of the pre- and post-flight analysis providing a better interpretation of experimental results and helping in the estimation of certain property values for the alloy. In this article an overview of the results, which were obtained as part of this numerical study is presented.

To avoid explicit tracking of the interface a fixed grid single domain approach was used to study unidirectional plane front solidification of a Bi-1 at% Sn alloy in a Bridgman furnace. In this approach the boundary conditions applied at the solid/liquid interface are replaced by source terms in the energy and solute conservation equations. This method was successfully used for directional solidification involving unsteady solidification and melting [2]. The model was then applied to the problem of simulating the MEPHISTO events. The problem involves heat conduction in the solid alloy and in the walls of the ampoule; heat and solute convection, and diffusion in the liquid. Solute diffusion in the solid is neglected. The effects of concentration-dependent melting temperature on the phase change processes are incorporated. Thermal conductivity differences between the solid and liquid phases and thermo-diffusion (Soret effect) are also taken into consideration.

The MEPHISTO-4 apparatus, shown schematically in Fig. 1, consists of three parallel tubes or ampoules (only one is shown in the figure), each containing Bi–Sn alloy, around which are placed two ‘furnaces’, each comprising

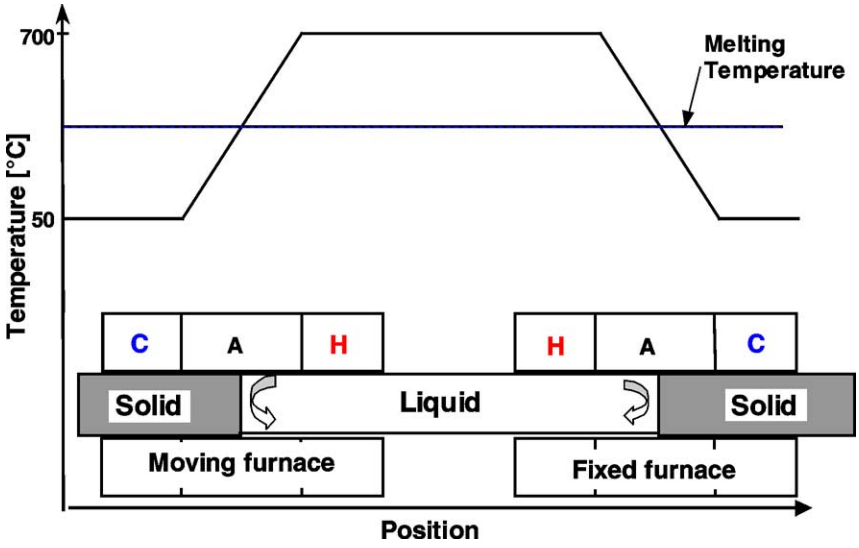

Fig. 1. Schematic diagram of the MEPHISTO apparatus. H and C denote the hot and cold sections of the furnaces; A denotes the adiabatic zone.

Fig. 1. Représentation schématique du dispositif MEPHISTO. H et C désignent respectivement les sections chaudes et froides du four et A la zone adiabatique.

[1] Matériel pour l’Étude des Phénomènes Intéressants de la Solidification sur Terre et en Orbite.

a pair of heating and cooling jackets. Between each heating and cooling jacket is a nominally adiabatic or insulated zone. One furnace is fixed and acts to generate a reference state; the other can be moved over the tubes in order to allow the solidification (or melting) of the material in the tube.

2. Mathematical formulation and numerical model

Taking into consideration thermo-diffusion (Soret effect) in the solute conservation equation the governing time-dependent equations describing momentum, heat and solute transport during unidirectional solidification of binary alloy are

$$\nabla \cdot \widetilde{V} = 0 \tag{1}$$

$$\rho\left(\frac{\partial \widetilde{V}}{\partial t} + \widetilde{V} \cdot \nabla \widetilde{V}\right) = -\nabla P + \nabla \cdot \left\{\mu\left[\nabla \widetilde{V} + \left(\nabla \widetilde{V}\right)^{\mathrm{T}}\right]\right\} + \widetilde{B} \tag{2}$$

$$\rho C_p\left(\frac{\partial T}{\partial t} + \nabla \cdot \left(\widetilde{V} T\right)\right) = \nabla \cdot (k \nabla T) + S_T \tag{3}$$

$$\frac{\partial C_l}{\partial t} + \nabla \cdot \left(\widetilde{V} C_l\right) = \nabla \cdot (D \nabla C_l) + D_T C_l (1 - C_l) \nabla^2 T + S_c \tag{4}$$

where ρ, μ, c_p, k, D and D_T are respectively the density, viscosity, specific heat and thermal conductivity of the alloy, the diffusivity of the solute and the thermo-diffusion coefficient. P, T, $\widetilde{V}$ and C are respectively the pressure, temperature, velocity vector and solute concentration. The source terms in the energy and solute equations take the place of the boundary conditions at the interface: $S_T = -\frac{\partial}{\partial t}(\rho f_l L)$ is used to account for latent heat release during phase change, and $S_c = \frac{\partial f_s}{\partial t}(1 - k_p) C_l + f_s \frac{\partial C_l}{\partial t}$ is added to the solute conservation equation to account for the release of solute into the liquid during solidification [2]. L is the latent heat and f_l is the local liquid fraction, k_p is the partition coefficient (C_s/C_l at the interface). For a partially solidified cell, a weighted average control volume conductivity is calculated from $k_{i,j} = k_l k_s/(f_s k_l + f_l k_s)$, where subscripts '$s$' and '$l$' refer to the solid and liquid phases. $\widetilde{B}$ is the body force term, in which the Boussinesq approximation is applied, viz. $\widetilde{B} = \rho_0[-\beta_T(T - T_0) + \beta_C(C - C_0)]\tilde{g}$, where β_T, β_C, ρ_0, T_0, C_0 and $\tilde{g}$ denote respectively the thermal and solutal expansion coefficients (assumed constant), the reference density, temperature and concentration, and the acceleration due to gravity. We have made the major simplifying assumption that a two-dimensional model will be adequate, an assumption which is justified by comparison between the calculations and experiments.

The computational domain comprises either 'liquid' or 'solid' or 'partially solidified' cells; it is only for the latter that the source terms are not zero. The exact location of the interface is not known a priori and must be determined as part of the solution process from the computed temperature and concentration.

When the induced concentration variations remain centred around a mean value C_0 the thermo-diffusion term in Eq. (4) can be simplified to $D_T C_0(1 - C_0)$ as in Garandet et al. [3] and in the case of dilute alloys to $C_0(1-C_0) \approx C_0$. Using H (the height of the ampoule), H^2/α (where α is the thermal diffusivity) and α/H as scale factors for length, time and velocity respectively, defining the non-dimensional temperature and concentration by $T' = (T - T_c)/\Delta T_r$ and $C' = C/C_r$ where $\Delta T_r = T_h - T_c$, and using primes to denote non-dimensional quantities, Eq. (4) can be written as

$$\frac{\partial C'_L}{\partial t'} + \nabla \cdot \left(\widetilde{V}' C'_L\right) = \frac{1}{Le}\left(\nabla^2 C'_L + Sr \nabla^2 T'\right) + S_C \tag{5}$$

where $Le = \alpha/D$ is the Lewis number and the non-dimensional Soret contribution is given by $Sr = (D_T/D)(C_0/C_r)\Delta T_r$. Eqs. (1)–(3) were non-dimensionalised in similar way. Details can be found in Timchenko et al. [2].

Eqs. (3) and (4) represent the fixed-grid approach for modelling heat and mass transfer during a phase change. An essential part of this approach is the derivation of an enthalpy–temperature–liquid fraction relationship.

Standard enthalpy methods are known to produce oscillations in temperature due to the fact that the nodal temperature of a partially solidified control volume is constant (equal to the melting temperature) while the liquid fraction, and hence the enthalpy is changing. To obtain a smooth history of the temperature and interface position and to account for the change in the temperature while the interface travels over the solidifying cell, the weighting procedure for estimating liquid fraction in a partially solidified control volume given in Timchenko et al. [4] was used.

During solidification, the melting temperature varies due to changes in solute concentration. With the assumption that phase change takes place under local thermodynamic equilibrium, the temperature at the interface, i.e., the melting temperature T_m, can be expressed as

$$T_m = T_{m0} + m_l C_I \tag{6}$$

where T_{m0} is the melting temperature of pure solvent (bismuth, in the case of MEPHISTO-4), m_l is slope of the liquidus, assumed to be constant and obtained from the phase diagram and C_I is the interface solute concentration in the liquid.

In a fixed-grid formulation the computed values of C_l obtained from Eq. (4) are liquid cell averaged values. As the interface moves from one cell to the next, this average value suddenly decreases because of the finite discretization. It then gradually increases as solidification proceeds due to solute rejection at the interface, which occurs (with Bi–Sn) at a rate faster than diffusion out of the control volume. It follows that the concentration-dependent melting temperature, if calculated from the average concentration, will have an incorrect zigzag shape and hence will not be suitable for the calculation of the local liquid fraction or for the estimation of interface position. To overcome this problem, concentration-dependent melting temperature was calculated based on the correct interface solute concentration extrapolated from the cell average values [4].

To be able to use an extrapolation scheme for concentration we need to obtain a smooth decrease in the temperature of the partially solidified cell as the interface moves through the cell. However, translation of an isothermal together with an adiabatic boundary condition does not generate a smooth change in the boundary temperature as the boundary cell is treated as either isothermal or adiabatic depending where the junction between the isothermal zone and the adiabatic zone lies with respect to the grid point. Because the boundary condition is implemented on discrete points, this change cannot take place continuously in time. Therefore in order to achieve a continuous translation of adiabatic boundary condition along a fixed grid boundary, a weighted boundary condition was used for the boundary cell containing this junction point [4].

3. Results and discussion

3.1. Comparisons with analytical solutions

To validate the physical and mathematical models, a comparison of numerical results (Cn) with the analytical solution (Ca) of Smith et al. [5] for one-dimensional, diffusion-controlled plane front solidification was performed. No convection was included. Results of this comparison are shown in Fig. 2. It can be seen that the computed solute concentrations in the solid at the mid-height of the ampoule are very close to the analytical, diffusion controlled values. The relative difference $(\mathrm{Ca} - \mathrm{Cn})/\mathrm{Ca}$ is less than 1%. As noted below, segregation occurs and the concentrations away from the mid-height would differ from these one-dimensional values. Fig. 2(b) shows liquid cell average concentration (solid line) and extrapolated interface concentration (dashed line), which was used to calculate the solid concentration shown in Fig. 2(a).

3.2. Modelling of MEPHISTO experiments

Computational solutions were obtained using two different methods: the commercial flow code CFX 4.2, which is based on a primitive variable–finite volume formulation, and a finite difference vorticity-stream function

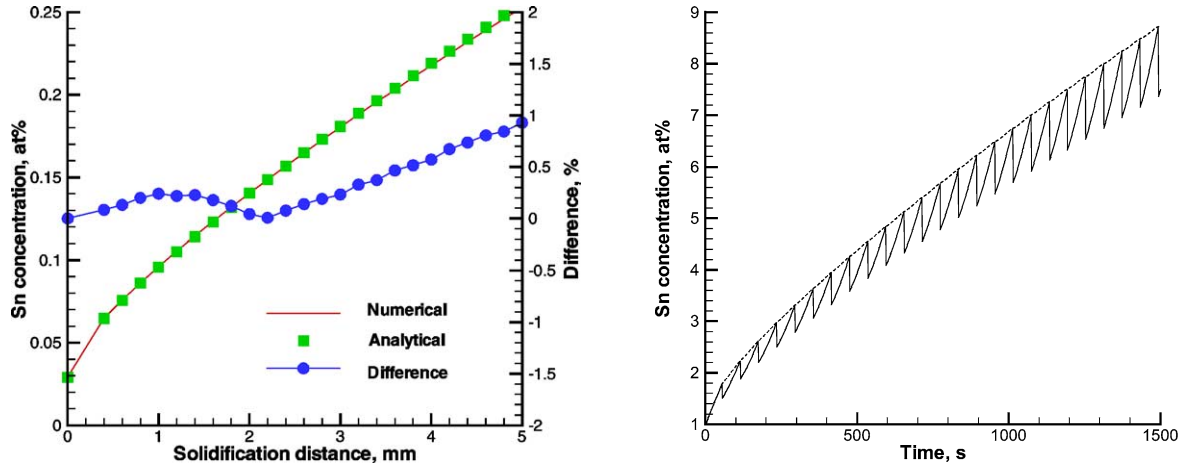

Fig. 2. (a) Analytical and numerical solute concentration in the solid for 5 mm of solidification; (b) time history of computed liquid cell average concentration (solid line) and extrapolated interface concentration (dashed line).

Fig. 2. (a) Profils analytique et numérique du champs solutal dans le solide pour 5 mm de matériau solidifié ; (b) histoire de la concentration moyenne d'une cellule de calcul (tracé continu) et concentration extrapolée à l interface.

formulation implemented in an in-house code called SOLCON. Details of these two methods and a comparison between results computed using each numerical method can be found in [4]. Results obtained from the two methods were in excellent agreement.

For the solutions presented here, grid sizes of 0.2 mm and 0.5 mm in the x (axial) and z (transverse) directions, and times steps of 1 s were typically used in CFX. For SOLCON grid size of 0.2 mm in the x and 0.3 mm in z directions was used with time step of 0.5 s. These mesh sizes were found to be adequate by testing against results obtained using finer meshes.

The model has been applied to the simulation of the experiments performed during the 1997 flight of MEPHISTO-4. In the example described below (the events identified in the flight schedule as 11E and 11F), solidification at a pulling speed (the speed of the moving furnace) of 3.34 μm/s occurred for 0.333 h. The furnace was then stopped for 3.7 hours (an 'extended hold') during which time almost complete rehomogenization of the liquid occurred. Solidification at a speed of 1.85 μm/s followed for 0.6 h. The melting temperature was calculated according to Eq. (6) with $m = -2.32$ K/at%. The magnitude of the gravity vector was taken to be 1 μg, i.e., 9.81×10^{-6} m s^{-2}, acting in a direction normal to the axis of the ampoule. The variation of the thermal conductivity between the solid and liquid phases was taken into account with $k_l = 12.4$ W/m K and $k_s = 6.5$ W/m K. Properties values for pure liquid bismuth taken at a reference temperature of 271.3 °C (the equilibrium melting temperature of Bi) were used. The partition coefficient k_p for Sn in Bi was taken to be 0.029. Diffusion coefficient $D = 2.0 \times 10^{-9}$ m^2/s was chosen after a comparison of numerical solutions with post-flight microprobe results for solute concentration in the solid (see Fig. 3).

The moving temperature profile imposed on the outer walls of the ampoule consisted of a cold zone ($T_c =$ 50 °C), an adiabatic zone and a hot zone ($T_h = 700$ °C). The length of the adiabatic zone was 20 mm, leading to an internal temperature gradient in the liquid of approximately 20 K/mm.

The distribution of solute concentration in the solid along the sample centre line is shown in Fig. 4(a). Numerical solutions are presented together with microprobe results obtained after the flight from the experimental samples. Fig. 4(b) shows the distribution of solute concentration across the solid. The major difference occurring in the presence of Soret effect is during the hold where the drop in concentration due to diffusion changes significantly. The Soret contribution gives a higher concentration in the interface vicinity during the hold because, with a very

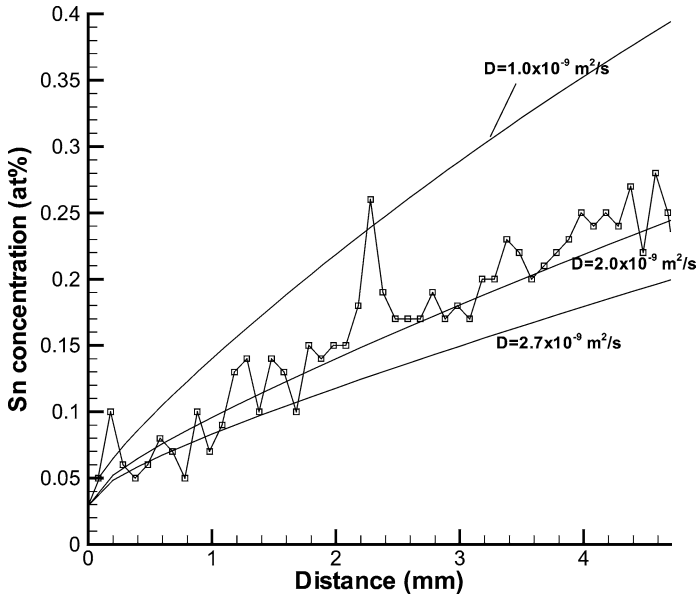

Fig. 3. Comparison of micro-probe experimental results with analytically predicted solid solute concentration for different diffusion coefficients.

Fig. 3. Comparaison des relevées expérimentaux aux prédictions analytiques du champs de concentration dans le solide pour différents coefficients de diffusion.

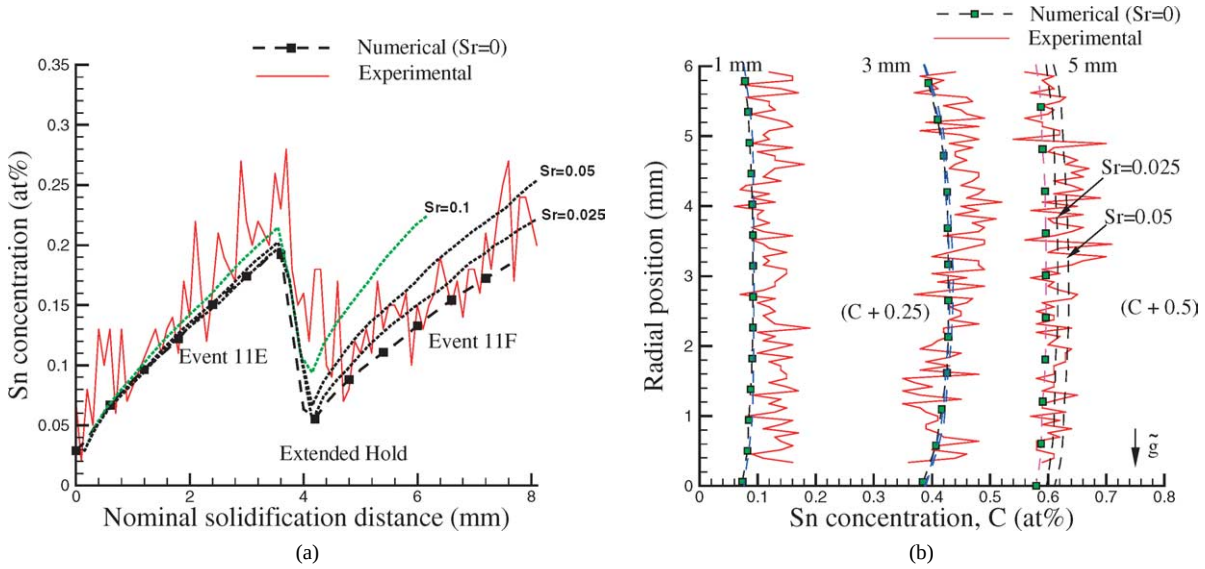

Fig. 4. Solid solute concentration: (a) along the ampoule centre line; and (b) across the ampoule.

Fig. 4. Concentration solutale : (a) le long de l'axe de l'ampoule ; (b) à travers l'ampoule.

small release of the solute, thermal diffusion becomes significant and being opposed to molecular diffusion causes an increase of solute at the interface. As the value of concentration at the end of hold is the initial condition for the second stage of solidification, the redistribution of solute during this second stage becomes quite different. As we can see, the results obtained for a Soret contribution of 5% gives the best agreement with the experimental results.

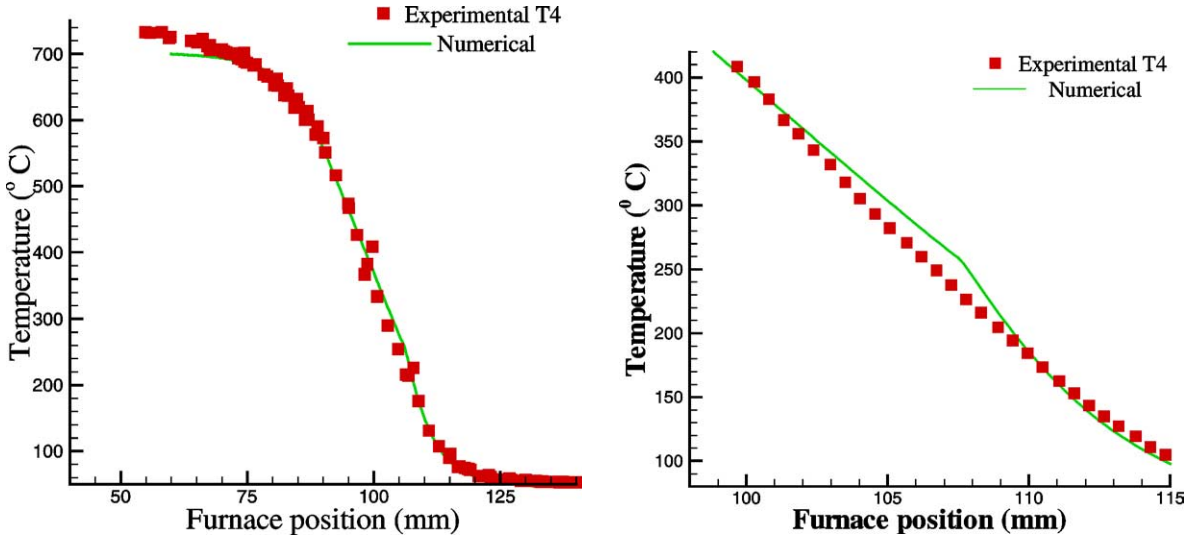

Fig. 5. Temperature distribution along: (a) the centre line; and (b) in the vicinity of interface.

Fig. 5. Distribution de température le long : (a) de l'axe de l'ampoule ; (b) au voisinage de l'interface.

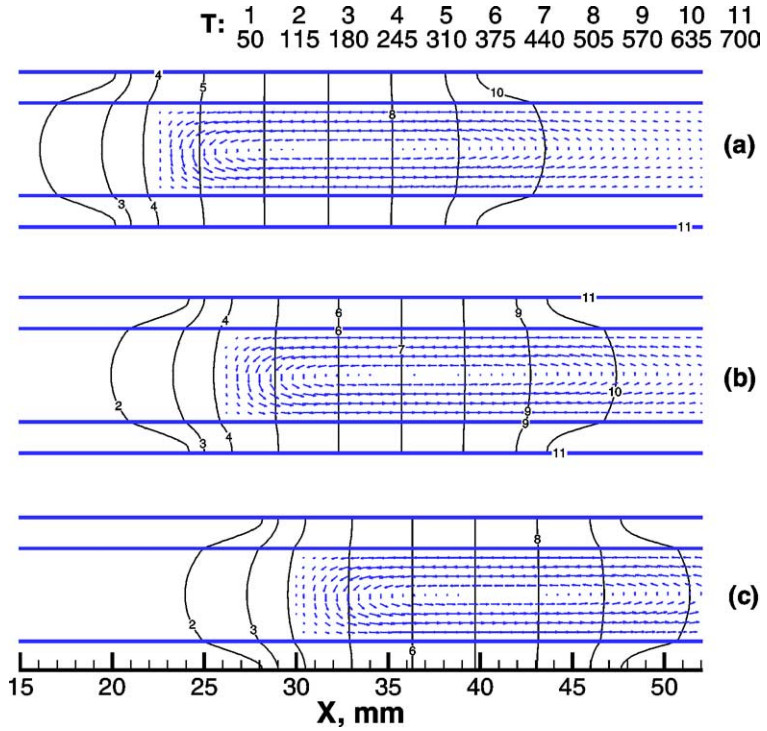

Fig. 6. Evolution of isotherms and fluid flow during solidification: (a) at the start of solidification; (b) at the end of event 11E; and (c) after event 11F.

Fig. 6. Évolution des champs thermique et dynamique durant la solidification : (a) au début du processus de solidification ; (b) à la fin de l'événement 11E ; (c) après l'événement 11F.

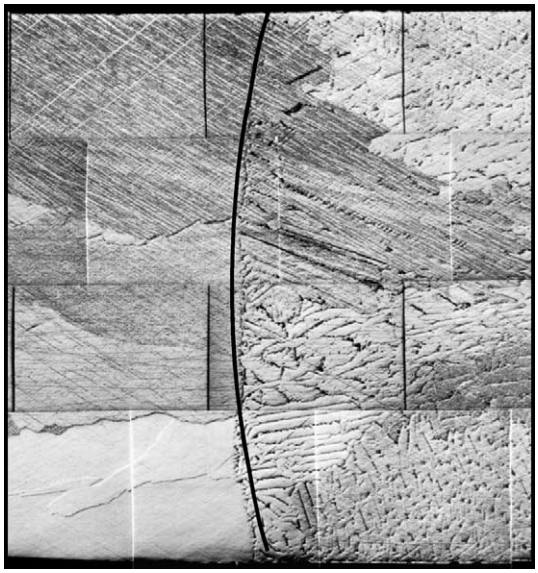

Fig. 7. Interface shape.

Fig. 7. Forme de l'interface.

Due to the limitation of how temperature was measured, some discrepancy did exist between numerical temperature predictions and actual measurements. Fig. 5(a) shows the computed temperature distribution along the centreline of the sample together with the in-flight measurements obtained using a thermocouple located on the centre line. Fig 5(a) contains measurement data obtained from all events, finer details of the temperature distribution in the vicinity of the interface taken from one event are shown in Fig 5(b). The change in the computed temperature gradient is caused by the change in thermal conductivity between the solid and liquid phases. The measurements do not exhibit this sharp change in the slope, a smearing of the experimental values is resulting from the finite size of thermocouple.

Fig. 6 shows evolution of isotherms and fluid flow during solidification (a) at the start of solidification, (b) in the end of event 11E and (c) after event 11F. It can be seen that both temperature and velocity fields are moving along the sample as time progresses according to the moving boundary temperature profile.

Fig. 7 shows the interface shape after the last event of solidification (11F) in MEPHISTO experiment. The predicted numerically interface shape is in excellent agreement with that observed in the actual experiment.

4. Conclusion

A modified fixed-grid approach has been used to simulate MEPHISTO experiments on solidification of a bismuth-tin alloy. To obtain smooth history of the temperature and interface position while interface is moving through a fixed-grid domain procedures for liquid fraction and interface concentration calculation were developed. Analysis shows that the numerical results with Soret contribution included are in a better agreement with the experimental result. The Soret effect could not be neglected especially if a hold is imposed on the furnace between the successive stages of solidification, because this modifies significantly the initial conditions and hence the following solidification stages. It has been shown that the higher increase of concentration in the vicinity of the solid/liquid interface in the presence of the Soret effect can be a cause of the morphological instability observed in the experiment.

Acknowledgements

The UNSW authors acknowledge with thanks the support of the Australian Research Council and the Australian Department of Industry, Science and Technology. They also express their gratitude to H.C. de Groh III, NASA Lewis Research Center, for the opportunity to participate in MEPHISTO-4 and his continual collaboration during this research.

References

[1] R. Abbaschian, H.C. de Groh III, E. Leonardi, G. de Vahl Davis, S. Coriell, G. Cambon, Final report for the shuttle flight experiment on USMP-4: In situ monitoring of crystal growth using MEPHISTO, NASA Technical Publication, NASA/TP-2001-210825, 2001.
[2] V. Timchenko, P.Y.P. Chen, G. de Vahl Davis, E. Leonardi, R. Abbaschian, A computational study of transient plane front solidification of alloys in a Bridgman apparatus under microgravity conditions, Int. J. Heat Mass Transfer 43 (2000) 963–980.
[3] J.P. Garandet, J.P. Praizey, S. Van Vaerenbergh, T. Alboussiere, On the problem of natural convection in liquid phase thermotransport coefficients measurements, Phys. Fluids 9 (1997) 510–518.
[4] V. Timchenko, P.Y.P. Chen, E. Leonardi, G. de Vahl Davis, R. Abbaschian, A computational study of binary alloy solidification in the Mephisto experiment, Int. J. Heat & Fluid Flow 23 (3) (2002) 258–268.
[5] V.G. Smith, W.A. Tiller, J.W. Rutter, A mathematical analysis of solute redistribution during solidification, Canad. J. Phys. 33 (1955) 723–743.